Effects of the molecule-electrode interface on the low-bias conductance of Cu–H_2–Cu single-molecule junctions

Zhuoling Jiang, Hao Wang, Ziyong Shen, Stefano Sanvito, and Shimin Hou'

Citation: J. Chem. Phys. **145**, 044701 (2016); doi: 10.1063/1.4959287
View online: http://dx.doi.org/10.1063/1.4959287
View Table of Contents: http://aip.scitation.org/toc/jcp/145/4
Published by the American Institute of Physics

Effects of the molecule-electrode interface on the low-bias conductance of Cu–H_2–Cu single-molecule junctions

Zhuoling Jiang,[1,2] Hao Wang,[1] Ziyong Shen,[1] Stefano Sanvito,[3] and Shimin Hou[1,4,a)]
[1]*Key Laboratory for the Physics and Chemistry of Nanodevices, Department of Electronics, Peking University, Beijing 100871, China*
[2]*Centre for Nanoscale Science and Technology, Academy for Advanced Interdisciplinary Studies, Peking University, Beijing 100871, China*
[3]*School of Physics, AMBER and CRANN Institute, Trinity College, Dublin 2, Ireland*
[4]*Beida Information Research (BIR), Tianjin 300457, China*

(Received 30 April 2016; accepted 11 July 2016; published online 22 July 2016)

The atomic structure and electronic transport properties of a single hydrogen molecule connected to both symmetric and asymmetric Cu electrodes are investigated by using the non-equilibrium Green's function formalism combined with the density functional theory. Our calculations show that in symmetric Cu–H_2–Cu junctions, the low-bias conductance drops rapidly upon stretching, while asymmetric ones present a low-bias conductance spanning the 0.2–0.3 G_0 interval for a wide range of electrode separations. This is in good agreement with experiments on Cu atomic contacts in a hydrogen environment. Furthermore, the distribution of the calculated vibrational energies of the two hydrogen atoms in the asymmetric Cu–H_2–Cu junction is also consistent with experiments. These findings provide clear evidence for the formation of asymmetric Cu–H_2–Cu molecular junctions in breaking Cu atomic contacts in the presence of hydrogen and are also helpful for the design of molecular devices with Cu electrodes. *Published by AIP Publishing.* [http://dx.doi.org/10.1063/1.4959287]

I. INTRODUCTION

Molecular electronic devices, with the potential to be the solution for electronics "beyond silicon," have aroused widespread attention during the past two decades.[1] The development of experimental techniques, such as mechanically controllable break junctions and scanning probe microscopy methods,[2,3] has made molecular electronics evolving from a theoretical hypothesis into an experimental reality. Thus great opportunities have opened up with the exciting possibility of manipulating quantum states, which are impossible to capture in conventional solid-state electronic devices. Among all the possible molecular junctions, a single hydrogen molecule bridging two metal electrodes is their prototype. The first of such junctions was reported by Smit *et al.*[4] In their experiment, a conductance plateau near 1 G_0 ($G_0 = 2e^2/h$ is the conductance quantum) was observed when platinum quantum point contacts were broken in a hydrogen atmosphere and the corresponding conductance histogram exhibited a sharp peak at 1 G_0 with a low conductance tail. Further theoretical investigations revealed that the 1 G_0 conductance is the result of the strong hybridization between the antibonding state of the H_2 molecule and the apex Pt atoms.[5] Afterward, considerable efforts have been devoted to the study of single hydrogen molecular junctions with coinage metal electrodes due to their much easier applications in molecular electronics.[6–15] However, most of these studies focused on Au/H_2 junctions, while only a few works have been reported for Ag and Cu atomic contacts, because no stable monatomic chains can be formed in the latter two cases. Recently, Kiguchi and co-workers investigated the electronic transport properties of Cu–H_2–Cu molecular junctions fabricated by breaking Cu atomic contacts in a hydrogen environment, and the conductance histogram showed a sharp 0.2–0.3 G_0 peak together with a clear 1 G_0 peak corresponding to the Cu atomic contacts.[11,12] To account for this observation, Motta *et al.* tentatively attributed the low-conductance state to a specific junction configuration in which one H_2 molecule sits laterally on the side of the Cu atomic contact.[13] The calculated conductance for such geometry is ~0.6 G_0, which is about twice as large as the experimental value.

The second important information for determining the geometry of the junction was also provided by Kiguchi and co-workers, who determined the vibrational energies of the Cu–H_2–Cu molecular junctions from the peaks of the differential conductance spectra.[11] They found that these vibrational energies are distributed in the 10-80 meV range with peaks at 20, 40, and 60 meV. They also suggested that the Cu–H_2–Cu molecular junctions should actually present asymmetric molecule-electrode interfaces, since the shape of the current-voltage (I-V) characteristics is itself rather asymmetric.[14] Although these experimental studies confirm the formation of Cu–H_2–Cu single-molecule junctions, the details of the atomic configuration and the conducting mechanism of Cu–H_2–Cu molecular junctions still remain elusive.

In order to address these important issues, we investigate the structural and electronic transport properties of a hydrogen molecule connecting to two Cu electrodes with different binding configurations by employing the non-equilibrium

a)Author to whom correspondence should be addressed. Electronic mail: smhou@pku.edu.cn

Green's function formalism combined with the density functional theory (that is the so-called NEGF+DFT approach).[16–25] Our calculations show that, as the electrode separation is increased, the low-bias conductance of the symmetric Cu–H_2–Cu junction with one H_2 molecule sandwiched between two identical pyramidal Cu tips drops rapidly. In contrast, the asymmetric Cu–H_2–Cu junction, in which the H_2 molecule is wired to one Cu electrode through a pyramidal Cu tip but binds at the hollow site of a pyramidal base on the surface of the other Cu electrode, can successfully reproduce the observed 0.2–0.3 G_0 conductance plateau. Moreover, the calculated vibrational energies of the asymmetric Cu–H_2–Cu junction are also distributed in the 20-80 meV range. Thus, the asymmetric Cu–H_2–Cu single-molecule junction is an appropriate junction model to explain both the low conductance plateau in the conductance curve and the distribution of vibrational energies observed for Cu atomic contacts broken in a hydrogen environment.

II. CALCULATION METHOD

In this work we use the SIESTA code to calculate the atomic structure of the Cu–H_2–Cu junctions and the quantum transport code SMEAGOL to study their electronic transport properties.[23–26] SIESTA is an efficient DFT package, in which the improved Troullier-Martins pseudopotentials are used to describe the atomic cores, while the wave functions of the valence electrons are expanded over a finite-range numerical orbital basis.[26,27] We adopt a double-zeta plus polarization basis set for all atoms, and the Perdew-Burke-Ernzerhof generalized gradient approximation for the exchange-correlation functional.[28] With our choice of pseudopotentials and basis functions, a lattice constant of 3.68 Å is obtained for bulk copper, in good agreement with the experimental value of 3.61 Å,[29] while the H–H bond length and the stretching frequency of the H_2 molecule in the gas phase are, respectively, calculated to be 0.75 Å and 4411 cm^{-1} consistent with the experimental values of 0.74 Å and 4401 cm^{-1}.[30,31] In the calculations, the Cu–H_2–Cu junctions are geometrically optimized until the atomic forces are smaller than 0.02 eV $Å^{-1}$. The Brillouin zone was sampled with a $4 \times 4 \times 1$ k-points mesh, and an energy cutoff of 250 Ry is used for the real-space integration mesh.

SMEAGOL is a practical implementation of the NEGF+DFT approach, which employs SIESTA as the DFT platform.[23–25] The unit cell of the extended molecule, where the scattering potential is computed self-consistently, comprises the hydrogen molecule, some Cu atoms with low coordination and ten Cu(111) atomic layers with a 3×3 in plane supercell. We always consider periodic boundary conditions in the plane transverse to the transport. The *I-V* characteristics of the Cu–H_2–Cu junction is calculated as

$$I = \frac{2e}{h} \int_{-\infty}^{+\infty} T(V,E)[f(E-\mu_L) - f(E-\mu_R)]dE, \qquad (1)$$

where $T(V, E)$ is the bias-dependent transmission function of the junction, $f(E)$ is the Fermi-Dirac distribution, and $\mu_{L/R} = E_F \pm eV/2$ is the local Fermi level of the left/right copper electrode with E_F being the Fermi energy. Then, the total transmission coefficient $T(V, E)$ of the junction is evaluated as

$$T(V,E) = \frac{1}{\Omega_{2DBZ}} \int_{2DBZ} T(\vec{k};V,E)d\vec{k}, \qquad (2)$$

where Ω_{2DBZ} is the area of the two-dimensional Brillouin zone (2DBZ) in the transverse directions. The k-dependent transmission coefficient $T(\vec{k}; E)$ is obtained as

$$T(\vec{k};E) = Tr[\Gamma_L G_M^R \Gamma_R G_M^{R+}], \qquad (3)$$

where G_M^R is the retarded Green's function matrix of the extended molecule and $\Gamma_{L(R)}$ is the broadening function matrix describing the interaction of the extended molecule with the left-hand (right-hand) side copper electrode. Here, we calculate the transmission coefficient by sampling 6×6 k-points in the transverse 2DBZ.

III. RESULTS AND DISCUSSION

We first explore the structural and the electronic transport properties of a symmetric Cu–H_2–Cu molecular junction, in which a hydrogen molecule is connected to two Cu(111) electrodes at each side through a four-atom Cu cluster arranged in a pyramid configuration and the H–H bond is along the transport direction (Fig. 1(a)). Figs. 1(b) and 1(c) display the evolution of the transmission coefficient at the Fermi level and some typical bond lengths in the junction as the electrode separation is increased. At each step, we relax the positions of the hydrogen molecule and the two pyramidal Cu clusters on the electrode surfaces, while keeping the copper atoms belonging to the electrodes fixed. The electrode separation L is defined as the distance between the outermost surface layers of the two electrodes. The starting point of the junction elongation is set to L = 12.70 Å and at this distance a nearly full open transmission channel is formed around E_F.[13] As we can see, there is a dramatic drop in the low-bias conductance during the junction stretching. Concomitantly, the bond length d_{H1-H2} of the hydrogen molecule contracts from 0.97 Å at L = 12.70 Å to 0.82 Å at L = 13.30 Å (note that the calculated gas-phase distance is 0.75 Å), whereas the distances d_{Cu1-H1} and d_{H2-Cu2} simultaneously increase from 1.87 Å to 2.30 Å. Considering the variations of these bond lengths upon elongation, we can conclude that the coupling between the H_2 molecule and the adjacent copper atoms is continuously weakened, thus resulting in a reduced transmitivity. Further stretching leads to an enormous increase in the bond length d_{H2-Cu2} and a slight decrease in the bond length d_{Cu1-H1} while d_{H1-H2} stays constant at 0.80 Å, which is close to the bond length of an isolated hydrogen molecule. This implies that the symmetric Cu–H_2–Cu molecular junction shown in Fig. 1(a) breaks up at the H2–Cu2 bond for L = 13.30 Å. We should note that due to its symmetric atomic arrangement, the Cu–H_2–Cu junction can break at either the Cu1-H1 bond or the H2–Cu2, one depending on the details of the relaxation process.[32]

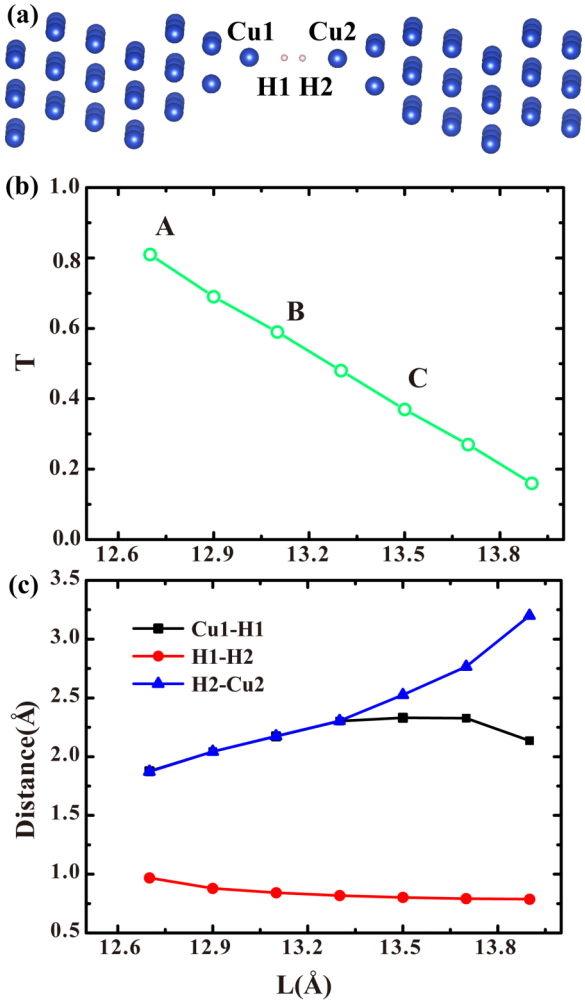

FIG. 1. (a) The optimized atomic structure of the symmetric Cu–H_2–Cu junction at the electrode distance L = 12.70 Å. The transmission coefficient at the Fermi level (b) and some typical bond distances (c) as a function of the electrode separation.

The equilibrium transmission spectrum of the symmetric Cu–H_2–Cu junction at the electrode separation of 12.70 Å, together with the local density of states (LDOS) projected onto the atomic orbitals of the hydrogen and apical copper atoms, is shown in Fig. 2. A noticeable transmission plateau appears around E_F. When comparing with the LDOS of the H and the apical Cu atoms in the junction, we find that the transmission plateau around E_F is dominated by the Cu 4s and H 1s atomic orbitals. This is also corroborated by the eigenchannel analysis,[33,34] which reveals that around E_F there is only one nearly full open conducting channel consisting of the Cu 4s and H 1s atomic orbitals (see Fig. S1 in the supplementary material).[35] In Fig. 2(d), we present the transmission spectrum projected onto the frontier molecular orbitals of the hydrogen molecule by using our previously developed scattering states projection method.[33] Similarly to the case of Pt–H_2–Pt molecular junctions,[5] the antibonding state of the hydrogen molecule hybridizes strongly with the adjacent Cu atoms and thus dominates the transmission around E_F. In contrast, the bonding state of the H_2 molecule yields a sharp transmission peak at −7.25 eV and makes a minor contribution to the transmission around E_F.

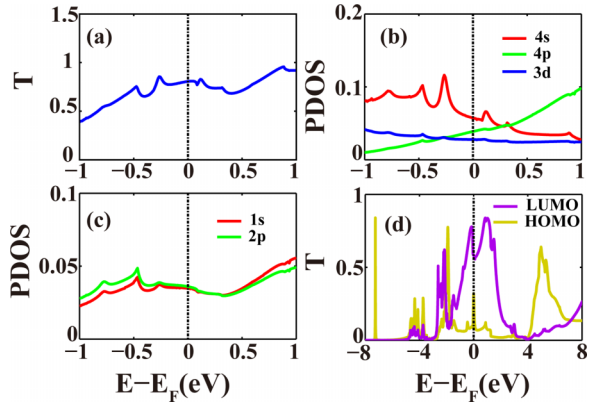

FIG. 2. The equilibrium transmission spectrum (a), the LDOS projected onto the 4s, 4p, and 3d atomic orbitals of the Cu2 atom (b), 1s and 2p atomic orbitals of the H2 atom (c), and the transmission projected onto the frontier molecular orbitals of H_2 (d) for the symmetric Cu–H_2–Cu junction at the electrode separation L = 12.70 Å.

The low-bias conductance of the symmetric Cu–H_2–Cu molecular junction drops rapidly following the increase of the electrode separation. When the junction conductance takes the value of 0.2–0.3 G_0, the symmetric Cu–H_2–Cu junction has broken at one of the two molecule-electrode interfaces (Fig. 1(c)). Therefore, the symmetric junction configuration cannot be responsible for the experimental observation of the 0.2–0.3 G_0 conductance plateau.[11,12] Since the *I-V* characteristics measured for the Cu–H_2–Cu junctions exhibits a prominently asymmetric shape, Kiguchi and co-workers claimed that the hydrogen molecule is asymmetrically bonded to the two copper electrodes.[14] Usually monatomic chains cannot be formed in Cu atomic contacts. Thus, when one Cu atomic contact breaks, the central single copper atom may remain on the surface of one Cu electrode forming a protruding single Cu atom whereas the other electrode ends with a smooth copper cluster on its surface. If a hydrogen molecule is trapped between these two electrodes thereafter, an asymmetric Cu–H_2–Cu molecular junction will be formed. We believe that this is the most likely geometry in breaking junction experiments.

In order to validate the above hypothesis, next we construct an asymmetric Cu–H_2–Cu junction model and investigate whether it can reproduce the 0.2–0.3 G_0 conductance plateau. When compared to the symmetric junction model shown in Fig. 1(a), the apex Cu atom in the pyramidal cluster on the surface of the right-hand side electrode is removed. Thus in our asymmetric Cu–H_2–Cu junction the H_2 molecule connects to a pyramidal Cu tip on the left-hand side but binds at the hollow site of a pyramidal base composed of three Cu adatoms on the right-hand one (Fig. 3(a)). Note that the distance between the electrodes is somehow an arbitrary quantity since in a real experiment it is set by the break junction setup. Here the initial electrode separation of the asymmetric Cu–H_2–Cu junction is chosen to be L = 10.77 Å. As shown in Fig. 3(b), the transmission coefficient at E_F of the asymmetric Cu–H_2–Cu junction is much reduced from that of the symmetric case, but it also decays rather slowly during the breaking process. Thus, the low-bias conductance of the asymmetric junction remains

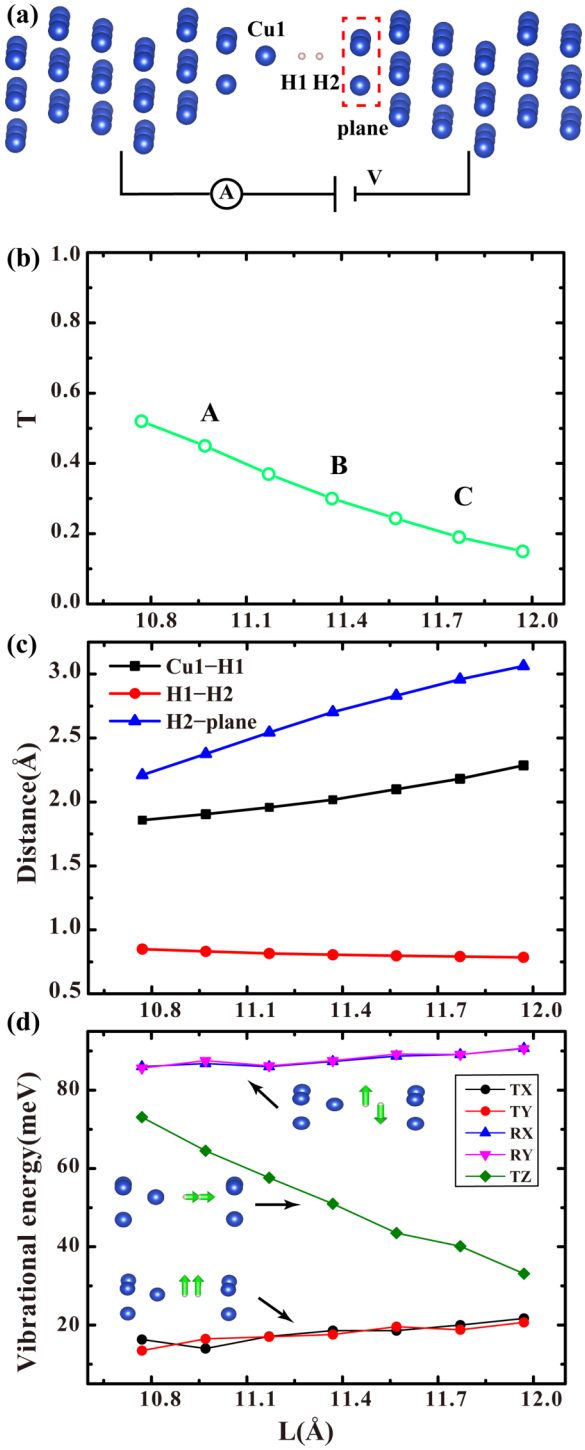

FIG. 3. (a) The optimized atomic structure of the asymmetric Cu–H_2–Cu junction at the electrode separation L = 11.37 Å. The transmission coefficient at the Fermi level (b), some typical bond distances (c) and the vibrational energies of the transverse vibration modes and the longitudinal translation mode of the two H atoms (d) as a function of the electrode separation.

in the 0.2–0.3 G_0 interval within a rather long range of electrode separations, in good agreement with the experiment results.[11,12,14] This marked difference between the asymmetric and symmetric junctions can be traced back to their different behaviors upon stretching. At variance with the symmetric Cu–H_2–Cu junction, where one Cu–H bond becomes longer but the other one becomes shorter as the electrode separation becomes larger than a certain value (Fig. 1(c)), in the asymmetric case the bond length d_{Cu1-H1} and the distance $d_{H2-plane}$ between the H2 atom and the plane constituted by the three Cu adatoms always get longer as the electrode separation is increased (Fig. 3(c)). Certainly, the major displacement of the two Cu electrodes occurs between the H_2 molecule and the three Cu adatoms. In detail, when the electrode separation is increased from 10.77 Å to 11.97 Å, the distance $d_{H2-plane}$ increases from 2.21 Å to 3.06 Å, while the bond length d_{Cu1-H1} is elongated by only 0.43 Å.

Because of the inelastic electron tunneling caused by electron-vibration interaction, experimental techniques such as action spectroscopy can measure the vibrational energies of a single-molecule junction and help us in characterizing the atomic configuration of the junction.[36] In order to further ascertain the suitability of the asymmetric Cu–H_2–Cu junction model, we have studied its dynamical properties. At variance with the gas phase in which only a stretching mode exists, the H_2 molecule in the asymmetric Cu–H_2–Cu junction has four types of vibration modes: the longitudinal stretching mode (ST), the longitudinal translation mode (TZ) with the center of mass of the H_2 molecule vibrating along the transport direction, the two transverse rotation modes (RX, RY) in which the angle between the H–H bond and the transport direction vibrates, and the two transverse translation modes (TX, TY) in which the center of mass of the H_2 molecule vibrates along the transverse directions. We calculate these vibration modes by using the frozen phonon method at each stretching step. Since the vibrational energy of the ST mode is around several hundreds meV, the observed vibration modes of Cu-H_2–Cu junctions can only be attributed to the other three types of molecular vibrations. As shown in Fig. 3(d), the calculated vibrational energies of the transverse translation modes are concentrated around 20 meV, while the vibrational energies of the transverse rotation modes are at about 85 meV, and all of these transverse vibration modes depend weakly on the electrode separation. In contrast, the vibrational energy of the longitudinal translation mode monotonically decreases from ~70 meV to ~30 meV as the electrode separation is increased from 10.77 Å to 11.97 Å, showing a strong dependence on the electrode separation. This is not a surprising result, considering that the longitudinal translation mode of the H_2 molecule in the asymmetric Cu–H_2–Cu junction depends sensitively on the molecule-electrode interaction. As the junction is elongated the binding energy between the H_2 molecule and the two Cu electrodes is weakened and thus the vibrational energy of the longitudinal translation mode becomes smaller. Thus, the vibration modes observed around 20 meV and 80 meV can be respectively assigned to the transverse translation and rotation modes, and the vibration modes observed between 30 meV and 70 meV can be assigned to the longitudinal translation mode. This good agreement between the calculated and experimental results provides a further support for the appropriateness of the asymmetric Cu–H_2–Cu junction model.[12]

Then we analyze the conducting mechanism of the asymmetric Cu–H_2–Cu molecular junction. Taking the junction with the electrode separation L = 11.37 Å as an example, we compare the equilibrium transmission spectrum

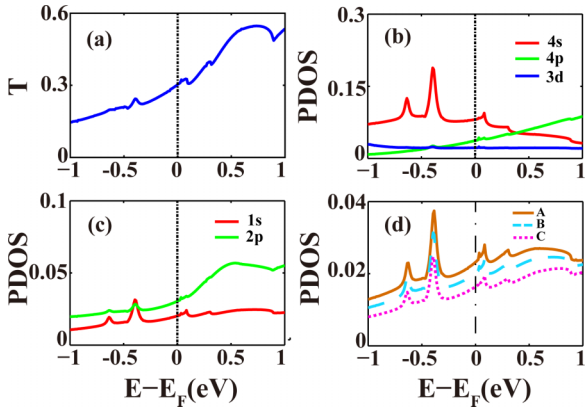

FIG. 4. The equilibrium transmission spectrum (a), the LDOS projected onto the 4s, 4p, and 3d atomic orbitals of the Cu1 atom (b), 1s and 2p atomic orbital of the H2 atom (c) of the asymmetric Cu–H_2–Cu junction at the electrode separation L = 11.37 Å. (d) The LDOS projected onto the 1s atomic orbital of the H2 atom at different electrode separations which are labeled in Fig. 3(b).

and the LDOS of the H and Cu atoms in the constriction. As shown in Fig. 4(a), a small transmission peak appears at −0.39 eV and extends above the Fermi level, resulting in a transmission coefficient of 0.30 at E_F. An analysis of the LDOS of the Cu1, H1, H2, and the three Cu adatoms, together with the calculation of the eigenchannels (see Fig. S2 in the supplementary material),[35] reveals that the transmission around E_F is dominated by the 4s orbital of Cu and the 1s of H. The dependence of the LDOS of the H2 1s atomic orbital on the electrode separation shows that, as the asymmetric Cu–H_2–Cu junction is stretched, the sharp peak centered at −0.39 eV and the LDOS around E_F have a small reduction, indicating that the coupling of the hydrogen molecule to the Cu electrodes is slightly weakened (Fig. 4(d)). As a result, the low-bias conductance of the asymmetric Cu–H_2–Cu junction shows a relatively weak decrease following the increase of the electrode separation. In contrast, in the symmetric Cu–H_2–Cu junction, the LDOS of the H2 1s atomic orbital presents a distinct decrease around E_F during the junction elongation (Fig. S3 in the supplementary material),[35] resulting in a dramatic drop of the zero-bias transmission.

Finally, we calculate the *I*-*V* curve of the asymmetric Cu–H_2–Cu molecular junction at the electrode separation L = 11.37 Å (Fig. 5(a)). As we can see, the electric current through the junction shows a clear dependence on the applied bias polarity and increases more rapidly at negative bias voltages. The asymmetry of the calculated *I*-*V* characteristics is rooted in the different coupling strengths at the two molecule-electrode interfaces, which can be appreciated from the bias-dependent transmission spectra (Fig. 5(b)). When a negative bias is applied to the left-hand side Cu electrode, which is decorated with a pyramidal Cu tip on its surface, the local Fermi level of that electrode shifts upwards, the transmission peak centered at −0.39 eV at zero bias is shifted to higher energies and the transmission around E_F is enhanced, resulting in a higher current. In contrast, when the bias polarity is reversed, the local Fermi level of the left-hand side Cu electrode shifts downwards, the same transmission peak is shifted to lower energies, and the transmission around E_F is on average diminished, resulting in smaller

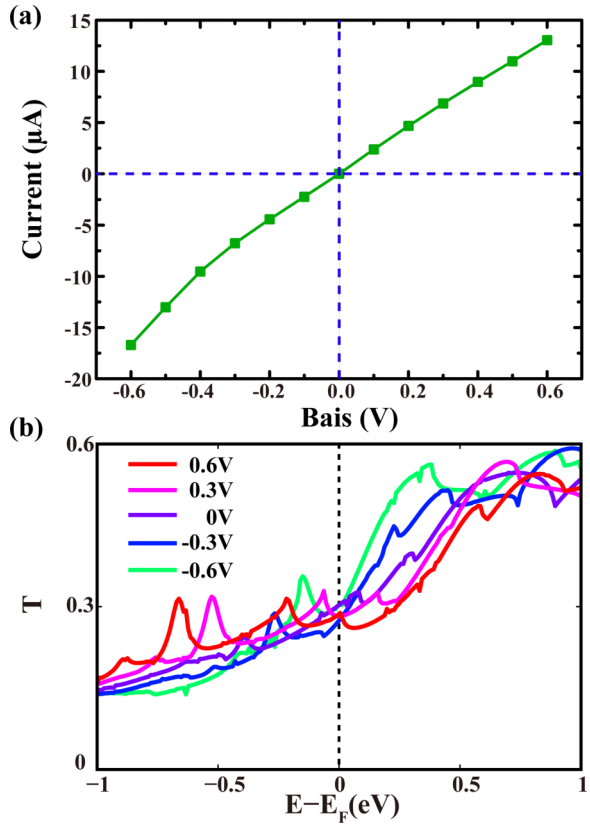

FIG. 5. The calculated *I*-*V* curve (a) and the bias-dependent transmission spectra (b) of the asymmetric Cu–H_2–Cu junction at the electrode separation L = 11.37 Å.

conductance. Therefore, the electronic coupling at the left-hand side molecule-electrode interface is stronger than that at the right-hand side one. Although the asymmetric shape of the *I*-*V* curve is successfully reproduced, the ratio between the calculated currents at the two bias polarities is less than that observed in experiments. In detail, the ratio between the currents calculated at ±0.6 V is only 1.3 whereas the measured value is 4.0 when the bias voltages are ±0.3 V.[14] This may be due to the too simplistic models of the Cu electrodes in our calculations and more complex asymmetric Cu electrodes are formed in real experiments.[14]

IV. CONCLUSION

In this study we have investigated the atomic structures and electronic transport properties of both the symmetric and asymmetric Cu–H_2–Cu junctions employing the NEGF+DFT approach. Our calculations show that the symmetric Cu–H_2–Cu junction presents a dramatic drop in conductance upon elongation and thus fails in reproducing the 0.2–0.3 G_0 conductance plateau measured in experiments. In contrast, an asymmetric junction shows a slowly descending conductance curve spanning the 0.2–0.3 G_0 range for long electrode separations. Vibrational analysis of the asymmetric Cu–H_2–Cu junction reveals that the vibrational energies of the transverse translation and rotation modes of the H_2 molecule, respectively, keep the nearly constant values of ~20 meV and ~85 meV at different electrode separations while

the longitudinal translation mode has vibrational energies around 30–70 meV, which are in good agreement with the experimental values. Therefore, the asymmetric Cu–H_2–Cu junction is the more preferred atomic configuration for single hydrogen molecules bonded to Cu electrodes. These findings not only provide an explanation to the observed vibrational and electronic transport properties of copper atomic contacts in a hydrogen environment but are also helpful in facilitating the design and fabrication of molecular electronic devices made with Cu electrodes.

ACKNOWLEDGMENTS

This project was supported by the National Natural Science Foundation of China (Grant Nos. 61321001 and 61271050) and the MOST of China (Grant No. 2013CB933404). S.S. thanks additional funding support from the European Research Council (QUEST project) and by AMBER (Grant No. 12/RC/2278).

[1]D. Xiang, X. Wang, C. Jia, T. Lee, and X. Guo, Chem. Rev. **116**, 4318 (2016).
[2]J. M. Krans, J. M. van Ruitenbeek, V. V. Fisun, I. K. Yanson, and L. J. De Jongh, Nature **375**, 767 (1995).
[3]B. Xu and N. Tao, Science **301**, 1221 (2003).
[4]R. H. M. Smit, Y. Noat, C. Untiedt, N. D. Lang, M. C. van Hemert, and J. M. van Ruitenbeek, Nature **419**, 906 (2002).
[5]K. S. Thygesen and K. W. Jacobsen, Phys. Rev. Lett. **94**, 036807 (2005).
[6]S. Csonka, A. Halbritter, G. Mihály, E. Jurdik, O. I. Shklyarevskii, S. Speller, and H. van Kempen, Phys. Rev. Lett. **90**, 116803 (2003).
[7]R. N. Barnett, H. Häkkinen, A. G. Scherbakov, and U. Landman, Nano Lett. **4**, 1845 (2004).
[8]S. Csonka, A. Halbritter, and G. Mihály, Phys. Rev. B **73**, 075405 (2006).
[9]T. Frederiksen, M. Paulsson, and M. Brandbyge, J. Phys.: Conf. Ser. **61**, 312 (2007).
[10]M. Kiguchi, T. Nakazumi, K. Hashimoto, and K. Murakoshi, Phys. Rev. B **81**, 045420 (2010).
[11]R. Matsushita, S. Kaneko, T. Nakazumi, and M. Kiguchi, Phys. Rev. B **84**, 245412 (2011).
[12]T. Nakazumi, S. Kaneko, and M. Kiguchi, J. Phys. Chem. C **118**, 7489 (2014).
[13]C. Motta, G. Fratesi, and M. I. Trioni, Phys. Rev. B **87**, 075415 (2013).
[14]Y. Li, S. Kaneko, S. Fujii, and M. Kiguchi, J. Phys. Chem. C **119**, 19143 (2015).
[15]Z. Jiang, H. Wang, S. Sanvito, and S. Hou, Phys. Rev. B **93**, 125438 (2016).
[16]Y. Meir and N. S. Wingreen, Phys. Rev. Lett. **68**, 2512 (1992).
[17]P. Hohenberg and W. Kohn, Phys. Rev. **136**, B864 (1964).
[18]W. Kohn and L. J. Sham, Phys. Rev. **140**, A1133 (1965).
[19]Y. Xue, S. Datta, and M. A. Ratner, Chem. Phys. **281**, 151 (2002).
[20]M. Brandbyge, J.-L. Mozos, P. Ordejón, J. Taylor, and K. Stokbro, Phys. Rev. B **65**, 165401 (2002).
[21]J. Zhang, S. Hou, R. Li, Z. Qian, R. Han, Z. Shen, X. Zhao, and Z. Xue, Nanotechnology **16**, 3057 (2005).
[22]R. Li, J. Zhang, S. Hou, Z. Qian, Z. Shen, X. Zhao, and Z. Xue, Chem. Phys. **336**, 127 (2007).
[23]A. R. Rocha, V. M. García-Suárez, S. W. Bailey, C. J. Lambert, J. Ferrer, and S. Sanvito, Nat. Mater. **4**, 335 (2005).
[24]A. R. Rocha, V. M. García-Suárez, S. Bailey, C. Lambert, J. Ferrer, and S. Sanvito, Phys. Rev. B **73**, 085414 (2006).
[25]I. Rungger and S. Sanvito, Phys. Rev. B **78**, 035407 (2008).
[26]J. M. Soler, E. Artacho, J. D. Gale, A. García, J. Junquera, P. Ordejón, and D. Sánchez-Portal, J. Phys.: Condens. Matter **14**, 2745 (2002).
[27]N. Troullier and J. L. Martins, Phys. Rev. B **43**, 1993 (1991).
[28]J. P. Perdew, K. Burke, and M. Ernzerhof, Phys. Rev. Lett. **77**, 3865 (1996).
[29]C. Kittel, *Introduction to Solid State Physics*, 8th ed. (Wiley, Hoboken, NJ, 2004).
[30]P. C. H. Mitchell, P. Wolohan, D. Thompsett, and S. J. Cooper, J. Mol. Catal. A: Chem. **119**, 223 (1997).
[31]D. A. Mcquarrie and J. D. Simon, *Physical Chemistry: A Molecular Approach* (University Science Books, Sausalito CA, 1997).
[32]D. Cakir and O. Gulseren, Phys. Rev. B **84**, 085450 (2011).
[33]R. Li, S. Hou, J. Zhang, Z. Qian, Z. Shen, and X. Zhao, J. Chem. Phys. **125**, 194113 (2006).
[34]M. Paulsson and M. Brandbyge, Phys. Rev. B **76**, 115117 (2007).
[35]See supplementary material at http://dx.doi.org/10.1063/1.4959287 for the eigenchannel analysis of symmetric and asymmetric Cu–H_2–Cu molecular junctions around the Fermi level, the LDOS projected onto the 1s atomic orbital of the H2 atom in the symmetric Cu–H_2–Cu junction at different electrode separations, and the dependence of the PDOS and transmission spectrum of the asymmetric Cu–H_2–Cu molecular junction as a function of the k-point integration mesh.
[36]Y. Kim, K. Motobayashi, T. Frederiksen, H. Ueba, and M. Kawai, Prog. Surf. Sci. **90**, 85 (2015).